Journal of Molecular Catalysis A: Chemical 307 (2009) 43–50

Contents lists available at ScienceDirect

Journal of Molecular Catalysis A: Chemical

journal homepage: www.elsevier.com/locate/molcata

Oxidative dehydrogenation of propane on silica (SBA-15) supported vanadia catalysts: A kinetic investigation

Arne Dinse[a], Sonia Khennache[a], Benjamin Frank[a], Christian Hess[b,c], Rita Herbert[b], Sabine Wrabetz[b], Robert Schlögl[b], Reinhard Schomäcker[a,*]

[a] Department of Chemistry, Technical University of Berlin, Straße des 17. Juni 124, Sekr. TC 8, D-10623 Berlin, Germany
[b] Department of Inorganic Chemistry, Fritz-Haber-Institute of the Max-Planck-Society, Faradayweg 4-6, D-14195 Berlin, Germany
[c] Eduard-Zintl-Institut für Anorganische und Physikalische Chemie, Technische Universität Darmstadt, Petersenstraße 20, D-64287 Darmstadt, Germany

ARTICLE INFO

Article history:
Received 6 August 2008
Received in revised form 21 January 2009
Accepted 6 March 2009
Available online 20 March 2009

Keywords:
Oxidative dehydrogenation
Propane
Supported vanadia catalysts
SBA-15
Kinetics

ABSTRACT

Silica (SBA-15) supported vanadium oxide was used for a kinetic study of the oxidative dehydrogenation of propane in a fixed bed reactor. Prior to this study, spectroscopic characterization using a variety of analytic techniques such as FTIR-, Raman-, DR UV–vis- and X-ray photoelectron spectroscopy revealed the absence of bulk vanadia and a high dispersion of active surface sites for the investigated catalyst. The kinetic data evaluation was based on a first order rate law. Calorimetric measurements were used to determine the heat of adsorption of propane on the catalyst.

The data indicate that the primary combustion of propane is negligible. Reaction orders of one for propane dehydrogenation and propene combustion indicate their participation in the respective rate-determining step. The zero reaction order determined for the catalyst reoxidation reveals participation of lattice oxygen in this reaction step. Higher activation energies of propane dehydrogenation as compared to propene combustion indicate the participation of the weaker allylic C–H bond of propene in the rate-determining step of the propene combustion. This results in higher propene selectivities at elevated temperatures. Kinetic parameters, including apparent and intrinsic activation energies and the equilibrium constant of propane adsorption allowed a comparison with theoretical predictions and show good agreement.

1. Introduction

Kinetic modelling is a powerful tool to elucidate reaction mechanisms in catalytic reactions. The resulting estimated kinetic parameters can also be used to experimentally verify theoretical DFT calculations. An interesting reaction for kinetic modelling is the oxidative dehydrogenation of propane (ODP) on supported vanadia catalysts [1–3]. Besides a great effort to describe these catalysts structurally [4–6] many studies tried to elucidate kinetics and mechanism of ODP [7–9]. A great disadvantage of all these studies is the lacking connection between kinetics and analytical characterization, the so called structure–reactivity relationship. The presence of bulk V_2O_5 on the catalyst surface, for example, which leads to unselective side reactions, could not be excluded in most of the mentioned studies. Furthermore, mass and heat transfer limitations were mostly not accounted for, making the provided kinetic data unreliable. For the kinetic description of ODP rate laws based on a Mars–van-Krevelen type reaction mechanism are often found [10–12]. However, first order rate expressions with respect to propane partial pressures may also be used for a sufficient experimental determination of turnover frequencies (TOF) and activation energies [13]. This study is based on a silica (SBA-15) supported model catalyst used for ODP in order to compare the mentioned parameters with those determined by quantum mechanical calculations [14,15], which were mainly done for silica supported vanadia clusters. The chosen catalyst has already been characterized in previous studies [16–18], which also take into account the influence of water on the dispersion of surface vanadium sites and describe the redox-behaviour of this catalyst via molecule probing in detail. The general reaction network for ODP, on which the kinetic modelling in this work is based, is depicted in Fig. 1. A parallel as well as a consecutive reaction is involved in the overall network. Propene is the desired product, whereas carbon oxides are generated via parallel combustion of propane or by secondary combustion of alkenes. The oxidation of CO towards CO_2 is rather slow and can usually be neglected [13].

* Corresponding author. Tel.: +49 30 31424973; fax: +49 30 31479552.
E-mail address: schomaecker@tu-berlin.de (R. Schomäcker).

1381-1169/$ – see front matter © 2009 Elsevier B.V. All rights reserved.
doi:10.1016/j.molcata.2009.03.008

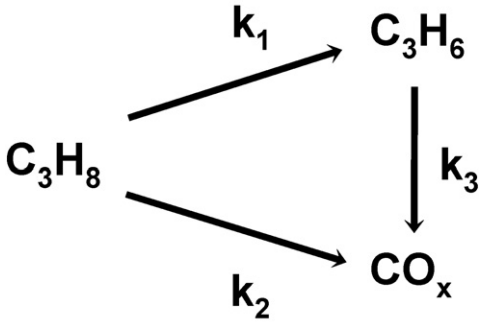

Fig. 1. Simplified reaction network of ODP.

2. Experimental

2.1. Catalyst preparation

Silica SBA-15 was synthesized according to Ref. [19]. Vanadium was incorporated via a multistep grafting-ion exchange procedure [17]. In the first step 6.4 ml of 3-aminopropyltrimethoxysilane (APTMS, Aldrich) was added to a stirred suspension of 2.5 g SBA-15 in 100 ml toluene and kept stirring for 12 h at 65 °C. Afterwards the suspension was filtered and washed with toluene to remove all free amine. In the second step the obtained dry powder was stirred in 150 ml of 0.3 M HCl for 12 h at room temperature. Subsequently it was filtered and washed with distilled water and dried at 110 °C overnight. In the third step the functionalized SBA-15 (2 g) was stirred in 60 ml water and 146 mg butylammonium decavanadate ($[BuNH_3]_6V_{10}O_{28}$, synthesized according to Ref. [20]) was added and the resulting mixture was stirred for 12 h at room temperature. The yellow content was filtered, washed and finally calcined for 12 h at 550 °C in air. The resulting content of vanadium was 2.7 wt%. The sample is hereafter denoted as V-SBA-15.

2.2. Calorimetric measurements

For calorimetric measurements, a Calvet calorimeter (MS70 SETARAM) has been combined with a house-designed high vacuum system, which enables the dosage of probe molecules within a range of 0.02 μmol. The pressure-controlled dosing systems allows the detection of adsorbed amounts of molecules (adsorption isotherm) as well as differential heat of adsorption and gives the possibility to elucidate the distribution of the adsorption sites along the range of adsorption heats [21].

The samples were pretreated and activated under mild conditions to minimize thermal and mechanical stress. All samples were pressed under low pressures (125 MPa; V-SBA-15 nearly stable up to 376 MPa [22], decrease of surface area (10%) of SBA-15 beyond 296 MPa [23]) and cut into small pellets, which were sieved to a diameter of 0.4–0.6 mm due to ultrahigh vacuum (UHV) conditions. The activation was conducted separately in the calorimetric cell connected to a turbomolecular-pump (Balzers). The activation was performed for 17 h at 373 K. The final pressure in the degassed cell was 10^{-6} mbar. The cell was cooled down to 313 K, placed inside the calorimeter and connected to the micro-calorimetric gas-adsorption system, subsequently. Propane 3.5 (Messer Griesheim) was dosed stepwise. Pressures (mbar), adsorption temperatures (°C) and the heat signals (V) were recorded.

2.3. Catalytic measurements

Experimental runs were carried out at temperatures between 673 and 773 K using u-shaped fixed bed quartz reactors at atmospheric pressure. For the measurements, catalyst samples between 200 and 900 mg in amount were portioned into the reactor. Using synthetic air as an oxygen source, propane and oxygen were fed in the ratio 1:1 ($C_3H_8/O_2/N_2$ = 16.9/16.9/67.5), 2:1 ($C_3H_8/O_2/N_2$ = 29.1/14.5/56.4) and 4:1 ($C_3H_8/O_2/N_2$ = 45/11.3/45) with a gas hourly space velocity (GHSV) of 6.6×10^2 to 6.6×10^3 h^{-1}. The propane conversion was kept below 10%, which enables isothermal and differential conditions. Mass transfer limitations were avoided using particle sizes of 200–300 μm. This is described in more detail elsewhere [24]. In addition, to check for diffusional limitations the Weisz modulus Ψ' considering propane as the limiting reactant was estimated. The Weisz modulus describes the ratio of reaction rate to reactant diffusion rate and is defined by Eq. (1):

$$\Psi' = L^2 \frac{m+1}{2} \frac{r_{\text{eff}} \rho_{\text{cat}}}{D_{\text{eff},C_3H_8} c_{C_3H_8}} \quad (1)$$

where L is the characteristic length of catalyst particle = 10^{-4} m; m is the reaction order of propane = 1; r_{eff} is the measured reaction rate = 6×10^{-3} mol s^{-1} kg^{-1}; ρ is the catalyst density = 2×10^3 kg m^{-3}; D_{eff} is the effective diffusivity = 10^{-5} m^2 s^{-1}; and c is the concentration = 8 mol m^{-3}.

With an effective rate of 6×10^{-3} mol s^{-1} kg^{-1} estimated for 500 °C, 10% propane conversion and the data given above a Weisz modulus of 0.15 is calculated indicating that the reaction proceeds much slower than the propane diffusion and no mass transfer limitation needs to be considered at 500 °C or lower temperatures.

Concentrations of the individual components were calculated from a GC analysis of the product gas and expressed in mol m^{-3}.

2.4. Parameter determination

Propane conversion X and propene selectivity S as functions of the respective concentration c_i were calculated from Eqs. (2) and (3):

$$X = 1 - \frac{c_{C_3H_8}}{c_{C_3H_{8,0}}} \quad (2)$$

$$S = \frac{c_{C_3H_6}}{c_{C_3H_{8,0}} - c_{C_3H_8}} \quad (3)$$

Initial reaction rates at low propane conversions were calculated according to Eq. (4):

$$r_0 = c_{0,C_3H_8} \frac{dX}{d\tau} \quad (4)$$

with r_0 being the initial reaction rate, c_0 the respective initial reactant concentration and τ the modified residence time calculated from catalyst mass and gas flow rate m_{cat}/F.

The ODP reaction network contains essentially the following parallel and consecutive reactions [25,26]:

$$C_3H_{8(g)} + \overset{+V}{V}O_{(s)} \rightarrow C_3H_{6(g)} + H_2O_{(g)} + \overset{+III}{V}_{(s)} \quad (A)$$

$$C_3H_{8(g)} + (4+3x)\overset{+V}{V}O_{(s)} \rightarrow 3CO_{x(g)} + 4H_2O + (4+3x)\overset{+III}{V}_{(s)} \quad (B)$$

$$C_3H_{6(g)} + (3+3x)\overset{+V}{V}O_{(s)} \rightarrow 3CO_{x(g)} + 3H_2O + (3+3x)\overset{+III}{V}_{(s)} \quad (C)$$

$$CO_{(g)} + \overset{+V}{V}O_{(s)} \rightarrow CO_{2(g)} + \overset{+III}{V}_{(s)} \quad (D)$$

$$O_{2(g)} + 2\overset{+III}{V}_{(s)} \rightarrow 2\overset{+V}{V}O_{(s)} \quad (E)$$

Homogeneous contributions to this reaction scheme were observed only at temperatures above 773 K.

Simplifications of Eqs. (A)–(E) are the following: (i) the conversion–selectivity trajectories presented in Fig. 2 have an

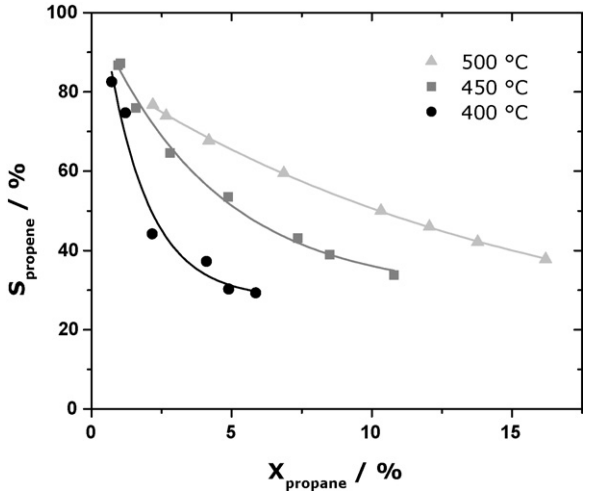

Fig. 2. Selectivity–conversion dependence of ODP at different temperatures for a SBA-15 supported vanadia catalyst.

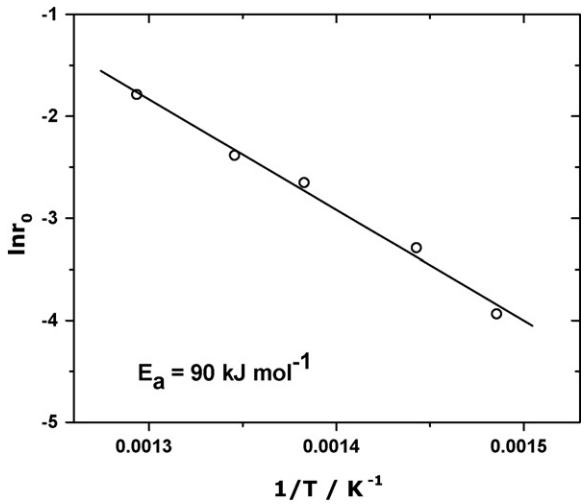

Fig. 3. Arrhenius plot for the determination of the activation energy of ODP.

extrapolated intercept at nearly 100% propene selectivity, indicating that primary propane combustion (B) can be neglected in this case and (ii) the ratio of CO and CO_2 was nearly constant at a value of 1.5, independent of the propane conversion. This indicates a slow CO oxidation to CO_2 and the reaction scheme simplifies to:

$$C_3H_{8(g)} + \overset{+V}{V}O_{(s)} \rightarrow C_3H_{6(g)} + H_2O_{(g)} + \overset{+III}{V}_{(s)} \quad (A)$$

$$C_3H_{6(g)} + 7\,\overset{+V}{V}O_{(s)} \rightarrow 2CO + CO_2 + 3H_2O + 7\,\overset{+III}{V}_{(s)} \quad (C1)$$

$$O_{2(g)} + 2\,\overset{+III}{V}_{(s)} \rightarrow 2\,\overset{+V}{V}O_{(s)} \quad (E)$$

Elimination of the catalytic species results in the stoichiometric equations for the stable compound, Eqs. (5) and (6):

$$C_3H_8 + 0.5O_2 \rightarrow C_3H_6 + H_2O \quad (5)$$

$$C_3H_6 + 3.5O_2 \rightarrow CO + CO_2 + 3H_2O \quad (6)$$

Please note that Eqs. (A)–(E) are based on the following assumption: one catalytic turnover leads to a reduction of vanadium (+5) to vanadium (+3). The assumption was made despite existing DFT calculations for silica supported vanadium oxide and bare V_2O_5 [14,15] predicting a lower activation barrier for reaction pathways only including a vanadium oxidation state of (+4). However, such mechanisms would not change the stoichiometry of Eqs. (5) and (6). Furthermore, reaction pathways including vanadium (+3) as short lived species could not be experimentally excluded so far.

The material balances for the stable reactants and products is given by:

$$\frac{dc_{C_3H_8}}{d\tau} = -r_1 \quad (7)$$

$$\frac{dc_{C_3H_6}}{d\tau} = r_1 - r_2 \quad (8)$$

$$\frac{dc_{O_2}}{d\tau} = 0.5r_1 - 3.5r_2 \quad (9)$$

Rate expressions for ODH and consecutive propene combustion r_1 and r_2, respectively are:

$$r_1 = k_{1,\mathrm{eff}} \exp\left(\frac{-E_{A1,\mathrm{app}}}{RT}\right) c_{C_3H_8}^{n1} c_{O_2}^{m1} \quad (10)$$

$$r_2 = k_{2,\mathrm{eff}} \exp\left(\frac{-E_{A2,\mathrm{app}}}{RT}\right) c_{C_3H_6}^{n2} c_{O_2}^{m2} \quad (11)$$

Numerical integration for data evaluation was done by using "Athena Visual Studio" Version 11.0 which uses the least square method for fitting.

For the determination of the equilibrium constants for the propane adsorption on V-SBA-15 a Langmuir equation was fitted a set of experimental data. The Langmuir isotherm is given in Eq. (12):

$$\frac{N}{N_0} = \frac{Kp}{1 + Kp} \quad (12)$$

with N the number of adsorbed molecules, N_0 the number of molecules for a monolayer coverage of the sample, p the pressure and K the equilibrium adsorption constant.The determination of the heat of adsorption was based on Eq. (13):

$$K = K_\infty \exp\left(\frac{\Delta H}{RT}\right) \quad (13)$$

with ΔH, the heat of adsorption.

3. Results

The grafting-ion exchange procedure used for the incorporation of vanadium into the porous silica matrix results in highly dispersed vanadia species [17]. For the sample used here (0.7 V nm^{-2}), no crystalline V_2O_5 was observed with visible Raman spectroscopy [16]. By combining Raman spectroscopy, DR UV–vis spectroscopy as well as X-ray photoelectron spectroscopy (XPS) we recently demonstrated the strong increase in the dispersion of the supported vanadia species upon dehydration [4]. The changes in the dispersion are accompanied by distinct structural changes, i.e., changes in the vanadium coordination as well as the size of the vanadia aggregates. Detailed studies using transmission IR spectroscopy with NO as probe molecule revealed the presence of bridged nitrates implying the presence of dimeric/polymeric vanadia species [18].

Fig. 2 shows the selectivity–conversion trajectories of V-SBA-15 as the function of temperature. It can be seen that the selectivity increases with temperature, indicating a weaker temperature dependence of propene combsution in comparison to propene formation by ODP, i.e., $E_{A1,app} > E_{A2,app}$.

Fig. 3 shows an Arrhenius plot for determination of the apparent activation energy of ODP from the initial rates of propane conversion. The calculated value of 90 kJ mol^{-1} can be used as an orientation for the subsequent determination of the kinetic parameters for the complete reaction network.

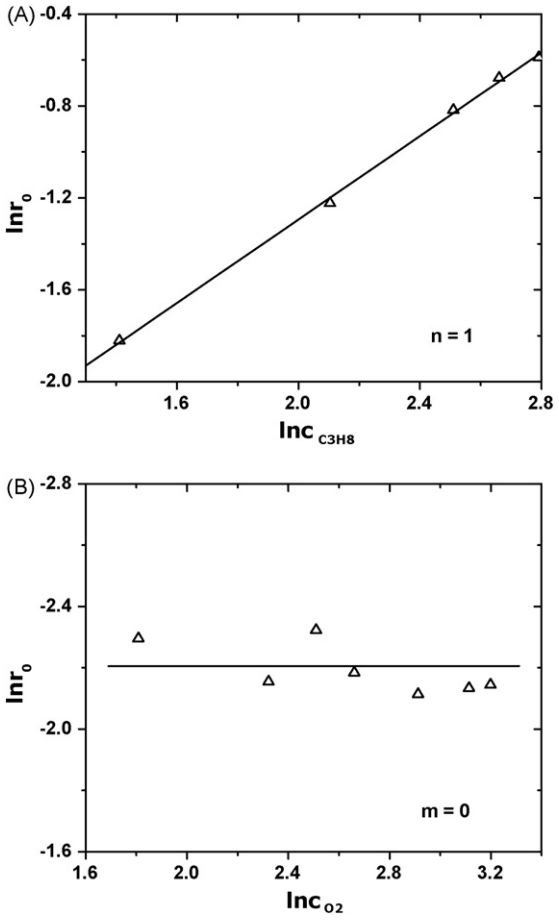

Fig. 4. Determination of the reaction orders for propane (A) and oxygen (B) in the dehydrogenation step.

The reaction orders for the oxidative dehydrogenation of propane were determined by a differential method studying the dependence of the initial rates on the individual initial concentration of the reactants. The logarithmic form of Eq. (10) yields Eq. (14):

$$\ln r_0 = \ln k_{\text{eff}} + n \ln c_{0,C_3H_8} + m \ln c_{0,O_2} \quad (14)$$

with r_0 the rate, $k_{1,\text{eff}}$ the effective rate constant, c_0 the respective reactant concentration, n the reaction order of ODP with respect to propane and m the order for oxygen, respectively. The reaction orders for propane and oxygen were determined by plotting the logarithm of the initial rate versus the logarithm of the concentration of the corresponding component. From the resulting slope the reaction orders were found to be 1 and 0 for propane and oxygen, respectively (Fig. 4).

The reaction orders of the consecutive reaction of propene and oxygen cannot be determined in terms of the particular partial reaction. This is because of propene being a stronger reducing agent than propane, resulting in a lower average oxidation state of the catalyst [24].

In order to get more insight into the consecutive propene combustion and its reaction orders an indirect method was used. This was done by considering the selectivity dependence on the conversion of ODP at different partial pressures of propane and oxygen. The propene selectivity dependence on the propane conversion indicates certain ratios of the reaction orders with respect to the reactants. If a change in the feed ratio of the substrates at the reactor inlet does not affect the selectivity towards propene, the consecutive reaction must be of an order of one and zero for propene and oxygen, respectively. If this is not the case, selectivity would vary strongly with the partial pressure of the reactant gas. For further allocation a simulation of the propene selectivity as a function of the propane conversion with different reaction orders for propane, propene and oxygen is depicted in Fig. 5.

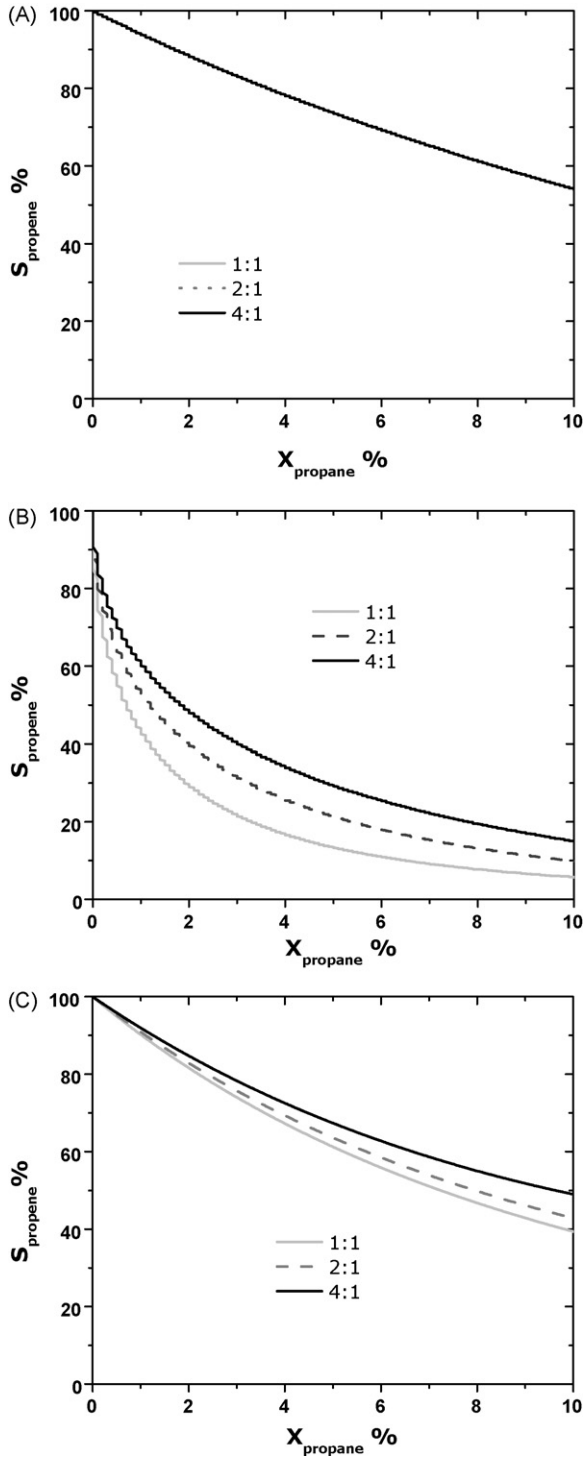

Fig. 5. Simulation of selectivity–conversion trajectories for ODP at 450 °C, for different reaction orders of propene and oxygen, respectively, in case of variable inlet concentrations of propane and oxygen. (A) Reaction order of one for propene and zero for oxygen, (B) reaction order of 0.5 for propene and zero for oxygen, (C) reaction order of 1 for propane and 0.5 for oxygen. Simulations were performed for 1 bar overall pressure and the partial pressures of the reactants chosen for the experiments.

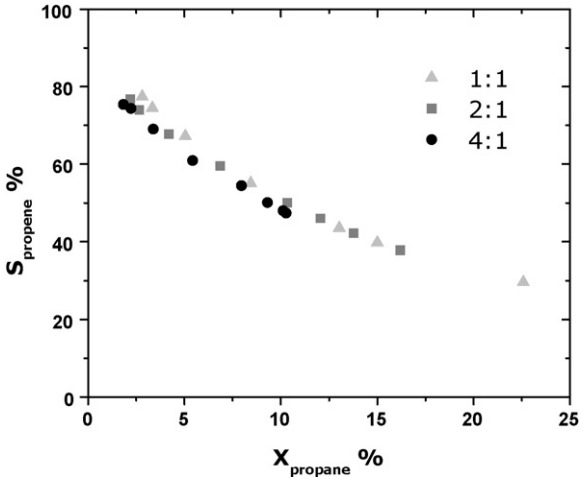

Fig. 6. Experimental selectivity–conversion dependence for different propane/oxygen ratios.

Table 1
Kinetic parameters for ODP reaction network.

x	$k_{0,\mathrm{eff},x}$ (ml mg^{-1} min^{-1})	$E_{\mathrm{A,app},x}$ (kJ mol^{-1})	n_x	m_x
1	2260 ± 1270	103 ± 6	1	0
2	0.7 ± 0.5	34 ± 18	1	0

Fig. 6 shows the measured selectivity–conversion trajectories for different initial concentrations of propane and oxygen. It can be seen that the propene selectivity is not affected by this variation. This leads to the conclusion that the reaction orders of the consecutive propene combustion are 1 and 0 for propene and oxygen, respectively, as shown by comparison with the simulation.

The experimentally determined reaction orders, discussed above, were subsequently implemented into the kinetic model for the reaction network, which consisted of a simple consecutive reaction of propane to propene and propene to carbon oxides and water. The respective equations are given in (10) and (11). The material balances for the stable compounds were fitted to experimental data at four different temperatures (673, 693, 723 and 773 K) and three different ratios of propane to oxygen (4:1, 2:1 and 1:1). Fitting variables were the apparent activation energies for ODP as well as for propene combustion and the respective pre-exponential factors $k_{1,\mathrm{eff}}$ and $k_{2,\mathrm{eff}}$.

The pre-exponential factors, reaction orders and apparent activation energies, determined by fitting the concentration profiles to the experimental data are depicted in Table 1.

Parity plots, shown in Fig. 7, indicate a good agreement of experimentally determined data and concentrations predicted by the derived model.

Fig. 8 shows the differential heats of propane adsorption at V-SBA-15 as well as at the pure SBA-15 support. For both materials similar adsorption enthalpies in the range of 40 kJ mol^{-1} were determined.

For the determination of the adsorption equilibrium constant, a Langmuir isotherm was fitted to a set of experimental data with variation of propane pressure. The results are depicted in Fig. 9.

As can be seen, the simulation is in very good accordance with the experimental data. The parameters determined for the propane adsorption are given in Table 2.

4. Discussion

Initial selectivities of almost 100% allow the conclusion that ODP is described by a simple consecutive reaction if SBA-15 supported

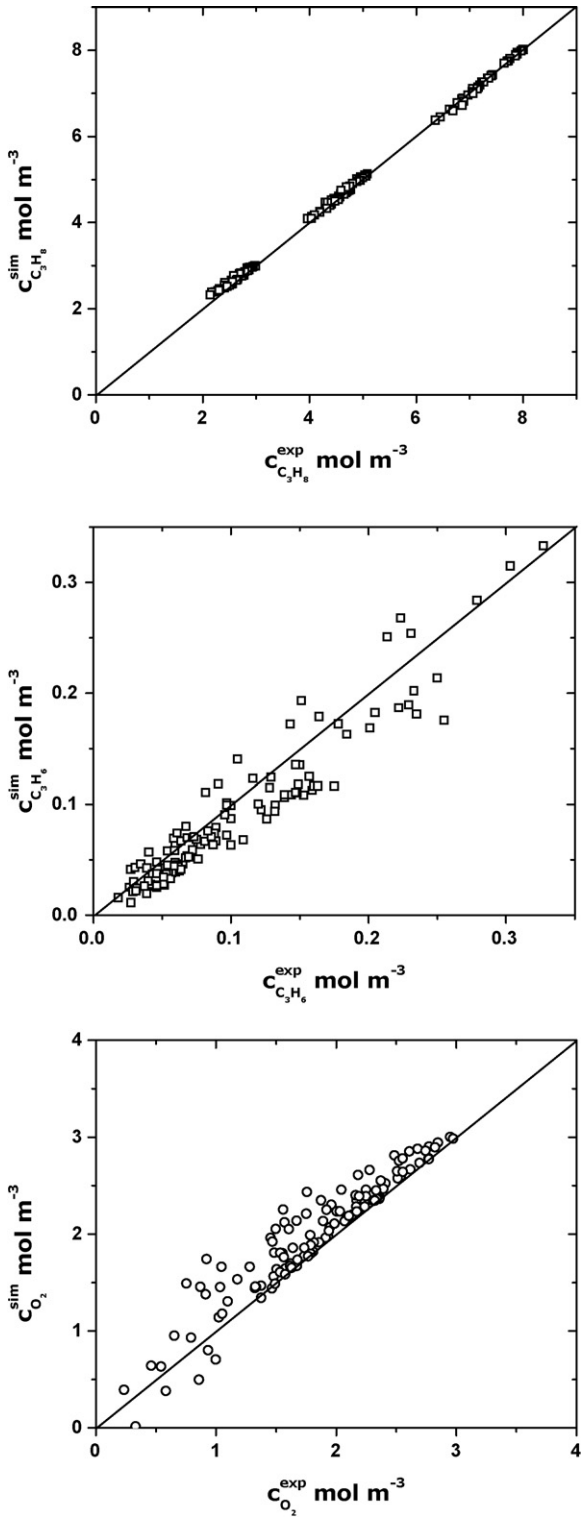

Fig. 7. Parity plots for simulated and experimental concentrations: (A) propane, (B) propene, and (C) oxygen.

Table 2
Thermodynamic parameters determined for the propane adsorption on V-SBA-15.

K_∞ ($\times 10^{-8}$ h Pa^{-1})	ΔH (kJ mol^{-1})
3.7 ± 0.4	40 ± 10

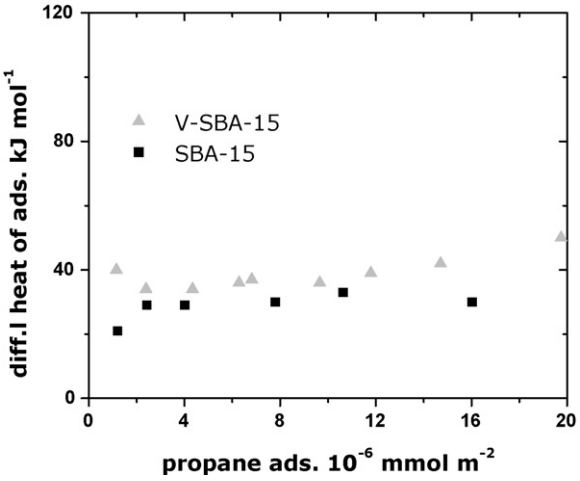

Fig. 8. Differential heats of adsorption as a function of adsorbed propane for SBA-15 (pure support) and V-SBA-15.

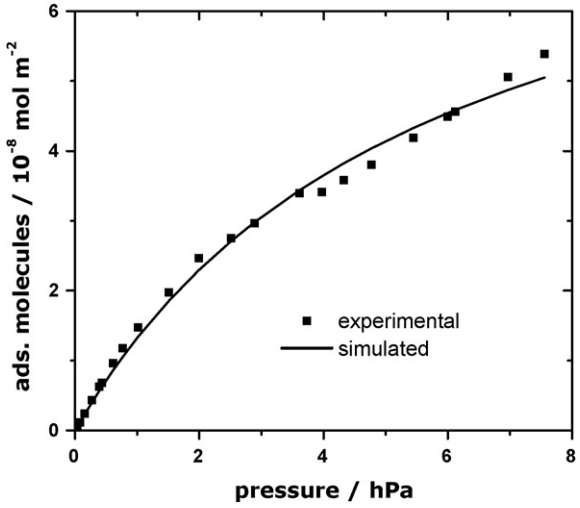

Fig. 9. Experimental data and simulation of the adsorption isotherm (Langmuir) of propane on V-SBA-15 at $T = 313$ K.

vanadium catalysts are used. The simplification of the reaction network leads to the chosen kinetic model described in Eqs. (10) and (11). A further important aspect concerning selectivity is the observation that it strongly increases with temperature. This was already found in a previous study for various other supported vanadia catalysts [24]. Only if the activation energy of oxidative dehydrogenation is higher than the activation energy of propene combustion, the rate of propene production increases stronger with temperature than the rate of the consecutive propene combustion, leading to a higher selectivity of the desired product. Therefore, a low activation energy is expected for the propene combustion, which is also in agreement with the lower bond strength of the allylic C–H bond (~370 kJ mol^{-1}) in propene compared to the stronger secondary C–H bond (~410 kJ mol^{-1}) in propane (Fig. 10).

Please note that the difference in the weakest C–H bond strength (40 kJ mol^{-1}) corresponds approximately to the difference in activation energies of ODP and propene combustion (70 kJ mol^{-1}) as calculated in this study.

The reaction order of one for the propane dehydrogenation indicates the participation of propane in the rate-determining step, which was already proven by isotopic tracer experiments done by Chen et al. [26] for different supported catalysts. In contrast, a zero order dependence as determined for gas phase oxygen proves that it is not involved in the rate-determining reaction step. This can only be the case if the reoxidation of the catalyst is fast compared to the reduction step involving the propane dehydrogenation. Such behaviour was also found in the case of other catalysts investigated in Refs. [10,25]. The reaction orders determined for the consecutive propene combustion of one for propene and zero for oxygen, respectively, suggest a participation of propene in the rate-determining step of the consecutive combustion. This may be explained by the similarity of the active C–H bond in both molecules. The good agreement of modelled and experimental data in Fig. 6 indicates that the assumptions made for the simplification of the reaction network are appropriate.

In order to calculate the intrinsic activation energies from the determined apparent activation energies, the elementary steps of ODP and the heat of adsorption of propane at the catalysts have to be known. According to isotopic tracer experiments done by Chen et al. [26], the elementary steps for one propane conversion to propene are the following:

1. Adsorption of propane on lattice oxygen:

$$C_3H_8 + O^* \overset{K_1}{\rightleftharpoons} C_3H_8O^* \quad \text{(r1)}$$

2. C–H bond abstraction from adsorbed propane involving a neighbouring oxygen atom:

$$C_3H_8O^* + O^* \xrightarrow{k_2} C_3H_7O^* + OH^* \quad \text{(r2)}$$

3. Desorption of propene:

$$C_3H_7O^* \xrightarrow{k_3} C_3H_6 + OH^* \quad \text{(r3)}$$

4. Formation of water under recombination of two neighbouring hydroxyl groups and formation of reduced vanadium centers depicted as *:

$$OH^* + OH^* \overset{K_4}{\rightleftharpoons} H_2O + O^* + * \quad \text{(r4)}$$

5. Reoxidation of the catalyst with gas phase oxygen:

$$O_2 + * + * \xrightarrow{k_5} O^* + O^* \quad \text{(r5)}$$

Their study revealed that the C–H bond abstraction of the secondary carbon atom in propane is the irreversible, rate-determining step in ODP and the overall rate of propane consumption can be derived from Eqs. (r1)–(r5) as a typical Mars–van-Krevelen rate law (Eq. (15)):

$$r_{C_3H_8} = \frac{k_2 K_1 c_{C_3H_8}}{\left(1 + \left((K_4 c_{H_2O})^{0.5} (k_2 K_1 c_{C_3H_8})^{0.25} / (2k_5 c_{O_2})^{0.25}\right)\right)^2} \quad (15)$$

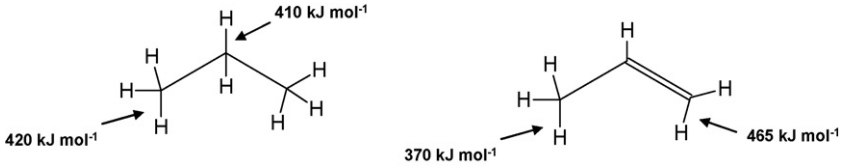

Fig. 10. C–H bond strength in propane (left) and propene (right).

Table 3
Literature data for ODP on silica supported vanadia.

x	$k_{x,0}$ (s^{-1})	$E_{A,app,x}$ ($kJ\,mol^{-1}$)
1	512 ± 56	70 ± 7
2	32,000 ± 3490	48 ± 5

Table 4
Comparison of experimentally and theoretically determined apparent activation energies.

Study	$E_{A,ODP}$ ($kJ\,mol^{-1}$)
This study	103 ± 6
Gilardoni et al.	112[a]
Rozanska et al.	123 ± 5

[a] Activation energy corrected by the heat of adsorption (40 $kJ\,mol^{-1}$).

where k_i is the respective rate constant and K_i the respective equilibrium constant for each reaction step (r1)–(r5). As found by Argyle et al. [27] by in situ-UV–vis spectroscopy, the reoxidation rate of the catalyst, described by k_5, is about 10^5 times higher than the rate-determining C–H bond abstraction, described by k_2 and K_1. Therefore Eq. (15) is simplified to Eq. (16):

$$r_{C_3H_8} = k_2 K_1 c_{C_3H_8} \quad (16)$$

This rate law is equal to Eq. (10) in the case of a zero order reaction of oxygen as determined in the experiments. Therefore, the simplified first order rate law, chosen for this study will result in the same kinetic description as a Mars–van-Krevelen type model. Because of the high reoxidation rate constant k_5, the kinetic parameters K_4 and k_5 cannot be determined accurately from a Mars–van-Krevelen model. A variation in these parameters has almost no impact on the rate of propane consumption. The product of k_2 and K_1 may also be written as:

$$k_2 K_1 = k_{2,0} \exp\left(\frac{-\Delta E_{A,2}}{RT}\right) K_{2,0} \exp\left(\frac{-\Delta H_{ads,2}}{RT}\right) \quad (17)$$

Thus, the measured apparent activation energy is the sum of the intrinsic activation energy of ODP and the heat of adsorption of propane on the active site. In order to calculate the intrinsic activation energies of ODP, the heats of adsorption of propane on V-SBA-15 were determined. The measured adsorption enthalpies indicate a weak interaction between propane and vanadium surface species. The above discussion leads to the conclusion that the intrinsic activation energy for ODP is approximately 140 $kJ\,mol^{-1}$.

Table 3 shows kinetic parameters determined by Grabowski and Sloczynski [28] for a high loaded silica supported vanadium catalyst. The apparent activation energy of the ODP is much lower (70 $kJ\,mol^{-1}$) than the values derived in this study (103 $kJ\,mol^{-1}$).

This fact may be attributed to the high vanadium loadings in the mentioned study, which lead to the formation of V_2O_5 for which the activation energy is actually measured. Furthermore, mass transfer limitations, which especially occur at high vanadium loadings, were not excluded. This makes the calculated kinetic parameters erroneous and leads to a lower activation energy for the ODP compared to the activation energy found in this study. The data, however also show, that the activation energy for the propene combustion is lower than that for ODP, as expected. Reaction orders were not determined in the study discussed above, because it was based on an Eley–Rideal mechanism, which implies a rate dependence according to the adsorption behaviour of the substrate.

The experimentally determined apparent activation energies of ODP are in good agreement with data derived from DFT calculations shown in Table 4 [14,15]. Theoretically determined values for propene combustion could not be found.

5. Conclusion

The SBA-15 supported catalyst used for this study is an ideal model catalyst, because of its well investigated characteristics and theoretically predictable reaction behaviour. However, further preparative studies are necessary to understand the difference between vanadium monomers and associated species. The reaction orders of one for oxidative dehydrogenation of propane and consecutive propene combustion indicate similar reaction mechanism for the activation of the two substrates. Higher activation energies of propane dehydrogenation as compared to the propene combustion indicate the participation of the weaker allylic C–H bond of propene in the rate-determining step of the propene combustion. In addition, this leads to higher propene selectivities at elevated reaction temperatures. A total oxidation of propane and propene with adsorbed molecular oxygen can be excluded, because in such a case a higher reaction order for ODP and propene combustion would then be expected. Zero reaction orders in the case of oxygen indicate a fast catalyst reoxidation for ODP and propene combustion. The fast reoxidation also justifies a first order rate law as a reliable method for the determination of the apparent activation energies. For further investigations of the reoxidation reactions transient experiments are needed. As shown by the calorimetric experiments, active vanadium sites have no influence on the adsorption behaviour of propane. The values of the heat of adsorption are in the expected range for surface reactions.

Acknowledgement

This work was supported by the German Research Foundation (Deutsche Forschungsgemeinschaft, DFG) through the corporate research center “Structure, dynamics and reactivity of transition metal oxide aggregates” (Sonderforschungsbereich 546, http://www.chemie.hu-berlin.de/sfb546). Christian Hess thanks the DFG for providing an Emmy Noether fellowship.

References

[1] M.A. Chaar, D. Patel, H.H. Kung, J. Catal. 109 (1988) 463–467.
[2] T. Blasco, A. Galli, J.M.L. Nieto, F. Trifiro, J. Catal. 169 (1997) 203–211.
[3] F. Cavani, N. Ballarini, A. Cericola, Catal. Today 127 (2007) 113–131.
[4] C. Hess, J. Catal. 248 (2007) 120–123.
[5] M. Inomata, K. Mori, A. Miyamoto, Y. Murakami, J. Phys. Chem. 87 (1983) 761–768.
[6] A. Khodakov, B. Olthof, A.T. Bell, E. Iglesia, J. Catal. 181 (1999) 205–216.
[7] S.L.T. Andersson, Appl. Catal. A 112 (1994) 209–218.
[8] R. Grabowski, J. Sloczynski, N.M. Grzesik, Appl. Catal. A 242 (2003) 297–309.
[9] K. Routray, K.R.S.K. Reddy, G. Deo, Appl. Catal. A 265 (2004) 103–113.
[10] K.D. Chen, A.T. Bell, E. Iglesia, J. Phys. Chem. B 104 (2000) 1292–1299.
[11] D. Shee, T.V.M. Rao, G. Deo, Catal. Today 118 (2006) 288–297.
[12] M.A. Vannice, Catal. Today 123 (2007) 18–22.
[13] B. Frank, A. Dinse, O. Ovsitser, E.V. Kondratenko, R. Schomäcker, Appl. Catal. A 323 (2007) 66–76.
[14] F. Gilardoni, A.T. Bell, A. Chakraborty, P. Boulet, J. Phys. Chem. B 104 (2000) 12250–12255.
[15] X. Rozanska, R. Fortrie, J. Sauer, J. Phys. Chem. C 111 (2007) 6041–6050.
[16] C. Hess, G. Tzolova-Muller, R. Herbert, J. Phys. Chem. C 111 (2007) 9471–9479.
[17] C. Hess, U. Wild, R. Schlogl, Micropor. Mesopor. Mater. 95 (2006) 339–349.
[18] T.V. Venkov, C. Hess, F.C. Jentoft, Langmuir 23 (2007) 1768–1777.
[19] D.Y. Zhao, Q.S. Huo, J.L. Feng, B.F. Chmelka, G.D. Stucky, J. Am. Chem. Soc. 120 (1998) 6024–6036.
[20] P. Roman, A. Aranzabe, A. Luque, J.M. Gutierrezzorrilla, Mater. Res. Bull. 26 (1991) 731–740.
[21] E.N. Coker, C.J. Jia, H.G. Karge, Langmuir 16 (2000) 1205–1210.
[22] R. Herbert, C. Hess, unpublished results.
[23] K. Cassiers, T. Linssen, M. Mathieu, M. Benjelloun, K. Schrijnemakers, P. Van Der Voort, P. Cool, E.F. Vansant, Chem. Mater. 14 (2002) 2317–2324.

[24] A. Dinse, B. Frank, C. Hess, D. Habel, R. Schomäcker, J. Mol. Catal. A 289 (2008) 28–37.
[25] A. Bottino, G. Capannelli, A. Comite, S. Storace, R. Di Felice, Chem. Eng. J. 94 (2003) 11–18.
[26] K.D. Chen, A. Khodakov, J. Yang, A.T. Bell, E. Iglesia, J. Catal. 186 (1999) 325–333.
[27] M.D. Argyle, K.D. Chen, E. Iglesia, A.T. Bell, J. Phys. Chem. B 109 (2005) 2414–2420.
[28] R. Grabowski, J. Sloczynski, Chem. Eng. Process 44 (2005) 1082–1093.